

Efficient optimization of cut-offs in quantum repeater chains

Boxi Li
ETH Zürich
Zürich, Switzerland
boxli@student.ethz.ch

Tim Coopmans
QuTech
Delft University of Technology
Delft, The Netherlands
t.j.coopmans@tudelft.nl

David Elkouss
QuTech
Delft University of Technology
Delft, The Netherlands
d.elkousscoronas@tudelft.nl

Abstract—Quantum communication enables the implementation of tasks that are unachievable with classical resources. However, losses on the communication channel preclude the direct long-distance transmission of quantum information in many relevant scenarios. In principle quantum repeaters allow one to overcome losses. However, realistic hardware parameters make long-distance quantum communication a challenge in practice. For instance, in many protocols an entangled pair is generated that needs to wait in quantum memory until the generation of an additional pair. During this waiting time the first pair decoheres, impacting the quality of the final entanglement produced. At the cost of a lower rate, this effect can be mitigated by imposing a cut-off condition. For instance, a maximum storage time for entanglement after which it is discarded. In this work, we optimize the cut-offs for quantum repeater chains. First, we develop an algorithm for computing the probability distribution of the waiting time and fidelity of entanglement produced by repeater chain protocols which include a cut-off. Then, we use the algorithm to optimize cut-offs in order to maximize secret-key rate between the end nodes of the repeater chain. We find that the use of the optimal cut-off extends the parameter regime for which secret key can be generated and moreover significantly increases the secret-key rate for a large range of parameters.

Index Terms—quantum communication, quantum repeater chains

I. INTRODUCTION

The realization of a quantum internet [1] will allow any two parties on earth to implement tasks that are impossible with its classical counterpart [2]. Quantum communication schemes rely on the transmission of quantum information, which in practice is precluded over long distances due to loss in the communication channel (usually glass fiber or free space). This problem can be overcome by dividing the distance between the sender and receiver of the quantum information into smaller segments, which are connected by intermediate nodes called quantum repeaters [3].

Most repeater schemes require quantum memories [4], [5]. Moreover, in many protocols an entangled pair is generated that needs to wait in a quantum memory until the generation of an additional pair. During this waiting time the first pair decoheres, reducing the quality of the final entanglement produced. At the cost of a lower rate, this effect can be mitigated by imposing a cut-off condition. For instance, a maximum storage time for entanglement after which it is discarded [6].

Cut-offs have been considered for entanglement generation in different contexts [6]–[17]. Notably, they play a key role for generating entanglement already in multi-pair experiments between adjacent nodes [8]. They also promise to be helpful in near-term quantum repeater experiments [9], [10], [14]. In the multi-repeater case, it is possible to obtain analytical expressions for the waiting time for general families of protocols [15], [16], though in general it appears challenging to extend those methods to characterize the quality of the states produced. Santra et al. [11] analytically optimized the distillable entanglement for a restricted class of quantum repeater schemes.

In this work, first we characterize the performance of a very general class of repeater schemes including cut-offs, probabilistic swapping, distillation and memory decoherence. We sidestep the challenge of analytical characterization by computing the probability distribution of the waiting time and fidelity of the first generated entangled pair between the repeater’s end nodes. For this, we improve the closed-form expressions by Brand et al. [18] to get faster algorithm runtimes and extend the expressions to repeater schemes which involve distillation and cut-offs. The runtime of the algorithm which evaluates these expressions is polynomial in the pre-specified size of the computed probability distribution’s support.

In the second part of the paper, we optimize the choices of the cut-off to maximize the secret-key rate. We find that the use of the optimal cut-off extends the parameter regime for which secret key can be generated and moreover significantly increases the secret-key rate for a large range of parameters. We also analyze the dependence of the optimal cut-off on different properties of the hardware and find that memory quality and the quality of the entanglement generated between adjacent nodes highly influence the effectiveness of the cut-off, whereas the influence is small for success probabilities of the individual repeater components. In addition, our numerical simulations show that for symmetric repeater protocols with evenly spaced nodes, a nonuniform cut-off (different cut-off time in different parts of the repeater chain) does not yield a significant improvement in end-to-end node secret key rate compared to a uniform cut-off.

This paper is organized as follows. In section II, we describe

the class of repeater schemes under study and elaborate on the hardware model used in our simulations. Section III presents the closed-form expressions and their evaluation algorithms for the waiting time distribution and output quantum states of repeater schemes which include cut-offs. The second part of the work, on optimization of the cut-off, consists of section IV, where we provide details on the optimization procedure, and the results of the numerical optimization as presented in section V. Section VI ends our work with a conclusion.

II. PRELIMINARIES

A. Class of repeater protocols considered

A quantum repeater chain connects two endpoints via several repeaters and aims to generate entanglement between the endpoints. In this section, we elaborate on the class of quantum repeater chain protocols we study in this work, which is an extension of the class studied in [18] with the addition of cut-offs. While doing so, we refer to both the endpoints and the repeater stations as nodes and to an entangled state between two nodes as a link.

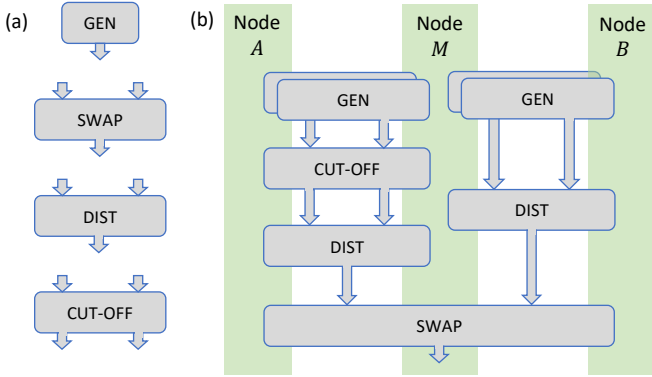


Fig. 1. The class of repeater chain protocols considered in this work are composed of four different types of PROTOCOL-UNITS. (a) The four PROTOCOL-UNITS: elementary-link generation between adjacent nodes (GEN), entanglement swapping for connecting two short-distance links in a single long-distance one (SWAP), entanglement distillation for converting two low-quality links in a single high-quality link (DIST) and discarding two links if their generation times differ by more than a pre-specified cut-off time (CUT-OFF). The algorithms provided in the article are applied to each PROTOCOL-UNIT individually (provided that each CUT-OFF is succeeded by a SWAP or DIST) and can thus be used to study repeater chain protocols which are composed of combinations of the four PROTOCOL-UNITS. The in-/outgoing arrows of each PROTOCOL-UNIT indicate the number of entangled links that the block consumes/produces. (b) An example of a composite protocol on three nodes (end nodes A and B and single repeater M). At the start of the protocol, two fresh elementary links are generated (GEN) in parallel between adjacent nodes A and M and subsequently selected through a CUT-OFF block. The first two links that survive the cut-off are then distilled (DIST) into a single link of higher quality. Asynchronously, the nodes M and B generate (GEN) pairs of links until the distillation (DIST) succeeds. Once distillation on both sides of node M has succeeded, the resulting links $A \leftrightarrow M$ and $M \leftrightarrow B$ are converted via a SWAP into a single entangled link between the end nodes A and B .

The class of quantum repeater protocols studied in this work are composed of the following four building blocks or PROTOCOL-UNITS: elementary link generation (GEN), entanglement swap (SWAP), entanglement distillation (DIST) and

cut-off (CUT-OFF). See fig. 1(a). All of these processes can fail, but the involved nodes receive a success or failure message. That is, they are heralded. In what follows, we describe these four PROTOCOL-UNITS in more detail and subsequently explain how they can be composed into a repeater scheme that spans multiple nodes.

The first block GEN represents the generation of fresh entanglement between two adjacent nodes. We refer to those entangled pairs as an elementary link. The GEN block thus spans precisely two nodes, takes no input and outputs a single link.

The second and third blocks are entanglement swap (SWAP) and entanglement distillation (DIST). In the setting of two nodes A and B with a middle station M in between, an entanglement swap [19] takes two links $A \leftrightarrow M$ and $M \leftrightarrow B$ and outputs a single link $A \leftrightarrow B$. It spans at least three nodes. Next, entanglement distillation probabilistically transforms two low-quality links between the same pair of nodes to a new one with higher quality [20], [21]. The DIST block thus spans at least two nodes, takes two links as input and outputs a single link, where each link is shared by the same pair of nodes. Both SWAP and DIST consist of local operations including measurements and classical communication. They can succeed or fail and in case of failure, both input links are lost.

The last PROTOCOL-UNIT is CUT-OFF, which takes two links as input (not necessarily between the same nodes). It declares ‘success’ in case the difference between the time at which those links were produced is smaller than some pre-specified cut-off time τ . In case of success, it leaves the two input links untouched and outputs them again. In case of failure, both input links are discarded.

We now explain how the four PROTOCOL-UNITS described above can be composed into a single repeater protocol spanning a chain of nodes. See fig. 1(b) for an example. Each composite protocol on a chain of nodes starts with one or multiple GEN blocks between each pair of adjacent nodes for fresh elementary link generation. A protocol then consists of stacking instances of the other three PROTOCOL-UNITS in such a way that the output link(s) of one are used as input link(s) to the other. The only restriction on how the PROTOCOL-UNITS can be stacked is that both output links of CUT-OFF are used as inputs for one DIST or SWAP block. As a consequence of the stacking, any repeater protocol in the class we study has a tree structure (see also fig. 1b). If a block at the root of a tree fails, then its input links are discarded and the GEN blocks at the tree’s leaves will restart.

We note that the class of repeater protocols described above includes, for instance, the well-known family of repeater schemes described by Briegel et al. [3], [22].

B. Model

We here describe how we model each of the four PROTOCOL-UNITS described in section II-A, which is identical to the modelling in [18], except for the newly introduced CUT-

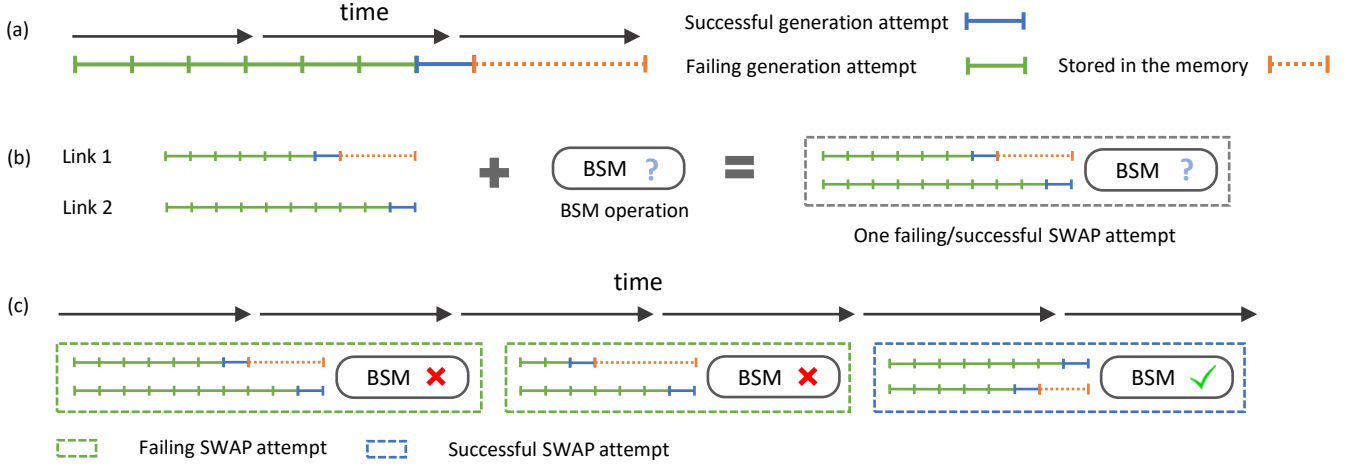


Fig. 2. Visualization of the waiting time until end-to-end entanglement is delivered for a 3-node repeater chain. The repeater scheme consists of the generation of two elementary links, followed by an entanglement swap on the two links. (a) A single link is generated in fixed-duration attempts, which succeed probabilistically and thus may fail (green line segment), after which generation is re-attempted until success (blue line segment). After that, the link is stored until it is consumed (dotted orange line segment). (b) A run of the 3-node protocol until the first swap attempt, which consists of first preparing two input links in parallel, followed by a Bell state measurement (BSM). The link that is generated earlier than the other needs to wait in the memory (link 1 in the figure, the ‘waiting’ is indicated by dotted orange line). While waiting, the earlier link’s quality decreases due to decoherence. The total waiting time before the BSM equals the maximum of the generation times of the two links. The BSM operation can fail, in which case the two links are lost and need to be regenerated. (c) A full run of the 3-node protocol, consisting of failed entanglement swaps (green dashed box) on fresh links until the first successful swap (blue dashed box). The total waiting time is the sum of the waiting times for the parallel generation of each pair of elementary links, up to and including the first successful swap.

OFF unit. For each PROTOCOL-UNIT, we describe the success condition as well as the quantum state that it outputs.

First, we model the fresh entanglement generation (GEN) using schemes which generate links in heralded attempts of duration $L_{\text{internode}}/c$, where $L_{\text{internode}}$ is the internode distance and c is the speed of light in the used transmission medium, e.g. glass fiber [4]. We assume that each attempt is independent and succeeds with constant probability $0 < p_{\text{gen}} \leq 1$. For simplicity, we assume that the nodes are equally spaced with internode distance L_0 , so that each attempt in elementary link generation takes duration $\Delta t_0 = L_0/c$, which will be the time unit in our numerical simulation.

We model the elementary link as a Werner state $\rho(w)$ with constant Werner parameter $w = w_0$ [23]:

$$\rho(w) = w |\Phi^+\rangle\langle\Phi^+| + (1-w) \frac{\mathbb{1}_4}{4} \quad (1)$$

where the Bell state

$$|\Phi^+\rangle = (|00\rangle + |11\rangle)/\sqrt{2} \quad (2)$$

is a maximally-entangled two-qubit state and

$$\mathbb{1}_4/4 = (|0\rangle\langle 0| + |1\rangle\langle 1|) \otimes (|0\rangle\langle 0| + |1\rangle\langle 1|) / 4$$

is the maximally-mixed state on two qubits. We refer to the parameter w with $0 \leq w \leq 1$ as the Werner parameter. Since a Werner state is completely determined by its Werner parameter, we use the Werner parameter to indicate the quantum state.

For the other three PROTOCOL-UNITs, the success conditions are summarized in table I. In short: we model entanglement swapping (SWAP) as succeeding with a constant

probability p_{swap} . For entanglement distillation, we use the BBPSSW protocol for entanglement distillation (DIST) [20] which we adapt by bringing the output state back into Werner form. The latter operation does not change the output state’s fidelity with the target state $|\Phi^+\rangle$. The success probability p_{dist} of distillation is a function of the input states’ Werner parameters (see [18] for details). The cut-off (CUT-OFF) success condition depends deterministically on the difference between the delivery times of its two input links, i.e. it succeeds when this difference is smaller than the cut-off time τ .

The states that the three other PROTOCOL-UNITs output are Werner states at any time of the execution of the protocol. Indeed, a successful entanglement swap or distillation attempt maps Werner states to Werner states (see [18] for a brief explanation). Also, the CUT-OFF leaves the input states untouched in case of success, thereby outputting Werner states if it got those as input. For each PROTOCOL-UNIT, the Werner parameters of the output links w_{out} are a function of those of the input links and are given in table I.

In addition to the fact that the PROTOCOL-UNITs change the quantum states they handle, the local quantum memories that are used to store the links are imperfect. In our model, a link with initial Werner parameter w , which lives in memory for time Δt until it is retrieved, decoheres to Werner parameter

$$w_{\text{decayed}} = w \cdot e^{-\Delta t/t_{\text{coh}}}. \quad (3)$$

where t_{coh} is the joint coherence time of the two involved memories.

For simplicity, we ignore the time needed for classical communication between the nodes in this work as well as the

time to perform the local operations. The algorithm we provide can be easily extended to include these features, following the extension described in [18].

In summary, for a given composite protocol (including the cut-off times τ for each CUT-OFF block), the simulation of the entanglement distribution process is determined by 4 hardware parameters: the success probability of elementary link generation p_{gen} , the swap success probability p_{swap} , the Werner parameter of the elementary link w_0 and the memory coherence time t_{coh} .

TABLE I
OVERVIEW OF SUCCESS PROBABILITY AND THE OUTPUT WERNER
PARAMETER FOR EACH PROTOCOL-UNIT

| PROTOCOL-UNIT | success probability p | Werner parameter w_{out} |
|---------------|---|---|
| generation | p_{gen} (constant) | w_0 |
| swap | p_{swap} (constant) | $w'_A \cdot w'_B$ |
| distillation | $p_{\text{dist}} = \frac{1 + w'_A w'_B}{2}$ | $\frac{w'_A + w'_B + 4w'_A w'_B}{6p_{\text{dist}}}$ |
| cut-off | $p_{\text{cut}} = 1, t_A - t_B \leq \tau$ $p_{\text{cut}} = 0, t_A - t_B > \tau$ | w'_A, w'_B |

where (t_A, w_A) and (t_B, w_B) are the waiting time and Werner parameter of the links A and B provided as input to the PROTOCOL-UNIT. The primed notation denotes Werner parameter with decay (eq. (3)) applied to the link that waits until the other is finished: $w'_X = w_X \cdot e^{-|t_A - t_B|/t_{\text{coh}}}$ if $t_X = \min(t_A, t_B)$ and $w'_X = w_X$ otherwise, for $X \in \{A, B\}$.

C. Waiting time and produced end-to-end state in repeater schemes using probabilistic components

In this work, we study the time until the first entangled pair of qubits is generated between the end nodes of the repeater chain (called ‘waiting time’ from here on) and the state’s quality, expressed as its Werner parameter (recall that the end-to-end state is a Werner state, see section II-B). Because the repeater chain protocols we study in this work are composed of probabilistic components, both the waiting time and the end-to-end state’s Werner parameter are random variables. For an illustration of the random behavior of the waiting time, see fig. 2. The algorithm we present in this work computes the probability distribution $\Pr(T = t)$ of the waiting time T and the average Werner parameter $W(t)$ of the end-to-end state which is delivered at time t .

Equivalently to the Werner parameter, we will express the state’s quality using the fidelity, which for general density matrices ρ and σ is defined as

$$F(\rho, \sigma) := \text{Tr} \left(\sqrt{\sqrt{\rho} \sigma \sqrt{\rho}} \right)^2.$$

The fidelity between a Werner state $\rho(w)$ and $|\Phi^+\rangle\langle\Phi^+|$ equals

$$F = \frac{1 + 3w}{4}.$$

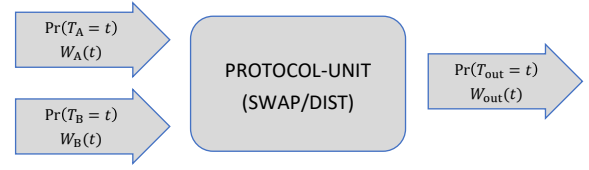


Fig. 3. The workflow of the algorithm for one PROTOCOL-UNIT (SWAP or DIST). It takes the waiting time distribution and Werner parameter of the two input links and computes those of the output.

III. COMPUTING THE WAITING TIME DISTRIBUTION AND OUTPUT WERNER PARAMETER

In this section, we present closed-form expressions of the waiting time probability distribution and Werner parameter of the output links for each PROTOCOL-UNIT, as function of waiting time distribution and Werner parameter of its input links. Expressions for a composite protocol are obtained by iterative application over the PROTOCOL-UNITs that the protocol consists of. These expressions naturally lead to an algorithm for their evaluation, which we also present in this section.

Closed-form expressions for GEN and SWAP were already obtained by Brand et al. [18], who explicitly mentioned that their approach does not generalize straightforwardly to DIST. Here, we include DIST and even CUT-OFF, provided the latter is succeeded by SWAP or DIST. The novel idea is to use separate expressions for the waiting time probability distribution of a successful and failed attempt. We then express the total waiting time distribution and the Werner parameter as those of the successful attempt averaged by the occurrence probability of all possible sequences of failed attempts, where the weighted average is efficiently computed using convolution. As additional benefit, the evaluation algorithm for SWAP is faster than the one presented by Brand et al.

In the following, we first derive general closed-form expressions for the waiting time distribution and Werner parameter of one PROTOCOL-UNIT in section III-A. We then give specific expressions for each PROTOCOL-UNIT individually in sections III-B to III-E. In the last section (section III-F), we show how these expressions can be converted into an efficient algorithm. We denote the random variables of the waiting time and average Werner parameter as T and $W(t)$, with subscript A and B for the input links or ‘out’ for the output link (see fig. 3).

A. General closed-form expressions for waiting time and produced states for all PROTOCOL-UNITs

1) *Random variable expression for the waiting time of PROTOCOL-UNITs:* We start by presenting an expression for the random variable T_{out} . To study the waiting time distribution, we divide the total waiting time into the waiting time for each attempt. An attempt can fail or succeed and it repeats

until the first successful attempt occurs (see fig. 2). The total waiting time T_{out} is given by

$$T_{\text{out}} = \sum_{i=1}^K M^{(i)} \quad (4)$$

where $M^{(i)}$ are i.i.d. random variables characterizing the waiting time of each attempt and therefore each is a function of the waiting time of two input links T_A, T_B . For example, for SWAP, we have $M = \max(T_A, T_B)$, i.e. we need to wait until both links are ready to perform the operation. K is the number of attempts we need until the first successful attempt occurs, which is also a random variable.

The success or failure of one attempt is characterized by a probability p . The success probability p of one attempt is independent of that of others and is given by $p = p(t_A, t_B, w_A, w_B)$ (table I). We reduce the Werner parameter dependence to time dependence by plugging in $w_A = W_A(t_A)$ and $w_B = W_B(t_B)$. Hence, we write $p(t_A, t_B)$ in the rest of this section.

The time dependence of p implies that, in general, K is correlated to $M^{(j)}$. To make this correlation between K and M in eq. (4) explicit, we introduce a random variable Y . Y denotes the binary random variable describing success (1) or failure (0) of a single attempt, subjected to the success probability $p(t_A, t_B)$. The time-dependent success probability can be understood as the success probability with given waiting time t_A, t_B of the input links:

$$p(t_A, t_B) = \Pr(Y = 1 | T_A = t_A, T_B = t_B).$$

We then rewrite eq. (4) with a sum over all possible number of attempts weighted by its occurrence probability [6]:

$$T_{\text{out}} = \sum_{k=1}^{\infty} \left\{ \left(Y^{(k)} \prod_{j=1}^{k-1} (1 - Y^{(j)}) \right) \cdot \sum_{i=1}^k M^{(i)} \right\}. \quad (5)$$

The expression in round brackets evaluates to 1 precisely if $Y^{(k)} = 1$ and $Y^{(j)} = 0$ for all $j < k$, and to 0 in all other cases. This factor thus makes that only the sum $\sum_{i=1}^k M^{(i)}$ is taken for which k is the first successful attempt. Notice that $Y^{(j)}$ and $M^{(i)}$ are correlated for all $i = j$ because they describe the same attempts. In the next section, we go further to compute the probability distribution of T_{out} .

2) *A closed-form expression for the waiting time distribution:* In the following, we give an expression of the waiting time distribution $\Pr(T_{\text{out}} = t)$ for one PROTOCOL-UNIT.

We consider the generation time of a successful or failed attempt separately and use the joint distribution of M and Y . We define the joint distribution that one attempt succeeds/fails and takes time t as

$$P_s(t) := \Pr(M = t, Y = 1) \\ = \sum_{t_A, t_B: \max(t_A, t_B) = t} \Pr(T_A = t_A, T_B = t_B) \cdot p(t_A, t_B), \quad (6)$$

$$P_f(t) := \Pr(M = t, Y = 0) \\ = \sum_{t_A, t_B: \max(t_A, t_B) = t} \Pr(T_A = t_A, T_B = t_B) \cdot [1 - p](t_A, t_B). \quad (7)$$

In the above equation, we iterate over all possible combinations of the input links' generation time t_A, t_B that leads to a waiting time t for this attempt.

With the definition eq. (6) and eq. (7), the sum of the waiting time for all attempts can be obtained by

$$\Pr(T_{\text{out}} = t) = \sum_{k=1}^{\infty} \left[\left(\bigstar_{j=1}^{k-1} P_f^{(j)} \right) * P_s \right](t) \quad (8)$$

where $*$ is the notation for convolution and the sum over k considers all the possible numbers of attempts. The notation $\bigstar_{j=1}^{k-1} P_f^{(j)}$ represents the convolution of $k - 1$ independent functions P_f . In the above equation, the discrete convolution is defined by

$$[f_1 * f_2](t) = \sum_{t'} f_1(t - t') \cdot f_2(t').$$

If f_1, f_2 describe two probability distributions of two random variables, their convolution is the distribution of the sum of those two random variables. However, neither P_f or P_s characterizes a random variable since they are joint distributions including Y . That is to say, P_s and P_f do not sum up to 1. Instead, we have

$$\sum_t P_f(t) + \sum_t P_s(t) = 1.$$

Therefore, the convolution here cannot be simply interpreted as a sum of two random variables. Instead, it is the summed waiting time conditioned on the success/failure of each attempt.

3) *A closed-form expression for the Werner parameter:* Here, we derive the expression for the Werner parameter $W_{\text{out}}(t)$.

To arrive at $W_{\text{out}}(t)$, we first compute the average Werner parameter of the output link of one attempt, given that it succeeds and finishes at time t :

$$W_{\text{suc}}(t) = \frac{\sum_{t_A, t_B: \max(t_A, t_B) = t} \Pr(T_A = t_A, T_B = t_B) \cdot [p \cdot w_{\text{out}}](t_A, t_B)}{P_s(t)}. \quad (9)$$

Here, w_{out} is the Werner parameter of the output link of a successful attempt and p the success probability (table I). Similar as in section III-A, we simplify the notation with $w_{\text{out}}(t_A, t_B) = w_{\text{out}}(t_A, t_B, W_A(t_A), W_B(t_B))$.

Next, we take a weighted average of W_{suc} over all possible sequences of failed attempts, followed by a single successful attempt:

$$W_{\text{out}}(t) = \frac{\sum_{k=1}^{\infty} \left[\left(\bigstar_{j=1}^{k-1} P_f \right) * (P_s \cdot W_{\text{suc}}) \right](t)}{\Pr(T_{\text{out}} = t)}. \quad (10)$$

where $\bigstar_{j=1}^{k-1} P_f^{(j)}$ computes the waiting time distribution of $k-1$ failed attempts and the additional convolution is the weighted average.

B. Specific case: GEN

We give here the expression for PROTOCOL-UNIT GEN. Since GEN does not have input links, the output does not rely on the expression introduced in the section III-A. Because one attempt in GEN takes one time step and the success probability p_{gen} is a constant, the waiting time can be described by a geometric distribution

$$\Pr(T_{\text{out}} = t) = p_{\text{gen}}(1 - p_{\text{gen}})^{t-1}.$$

The output state is a Werner state with Werner parameter w_0 as described in section II-B.

C. Specific case: SWAP

For entanglement swap, since p_{swap} is constant, Y is not correlated with M . As a result, P_s and P_f differ only by a constant coefficient (see eq. (6) and eq. (7)). Therefore, we can factor the constant out and get

$$\Pr(T_{\text{out}} = t) = \sum_{k=1}^{\infty} p_{\text{swap}}(1 - p_{\text{swap}})^{k-1} \left[\bigstar_{j=1}^k m \right] (t)$$

where

$$m(t) := \Pr(M = t) = \sum_{t_A, t_B: \max(t_A, t_B) = t} \Pr(T_A = t_A, T_B = t_B).$$

This is exactly the geometric compound distribution obtained in [18].

For the Werner parameter, we can directly use eq. (10) and obtain

$$W_{\text{out}} = \sum_{k=1}^{\infty} p_{\text{swap}}(1 - p_{\text{swap}})^{k-1} \left[\left(\bigstar_{j=1}^{k-1} m \right) * (m \cdot W_{\text{suc}}) \right] (t). \quad (11)$$

Compared to the expression in [18], this expression replaces the iteration over all pair of possible input Werner parameters for each k by convolution and therefore reduces the complexity (see section III-F).

D. Specific case: DIST

For entanglement distillation, the success probability depends on the Werner parameters. As discussed in section III-A, we can compute T_{out} and W_{out} because we iterate over all possible combinations of t_A and t_B and we use $W(t)$ to reduce the dependence on Werner parameters to the dependence on the waiting time. The calculation goes as follows. First, we compute P_f and P_s using $p(t_A, t_B) = p_{\text{dist}}(W(t_A), W(t_B))$ (table I). Then, we plug in P_f and P_s in eq. (8) to compute T_{out} . Finally, W_{out} can be calculated similarly using table I, eqs. (9) and (10).

E. Specific case: CUT-OFF

In the following, we show the specific expressions for CUT-OFF. CUT-OFF selects the input links and rejects them if one of the links is stored in memory for a time longer than the cut-off time τ . We consider only the case where CUT-OFF is followed by SWAP or DIST, so that the two blocks together output a single entangled link.

1) *The waiting time distribution:* We first introduce some additional notation to describe cut-off. We define a new binary variable for one attempt in preparing two links:

$$Y_{\text{cut}} = \begin{cases} 1 & \text{if } |T_A - T_B| \leq \tau \\ 0 & \text{if } |T_A - T_B| > \tau \end{cases} \quad (12)$$

We also define the waiting time of one cut-off attempt as Z , in contrast to M for a swap or distillation attempt. For CUT-OFF, we need to distinguish the waiting time of a successful and a failed attempt since they are not the same. In the case of failure, $Z_f = \min(T_A, T_B) + \tau$, because there is no need to wait for the second link longer than τ . In the case of success, we have $Z_s = \max(T_A, T_B)$.

Similar as the nested structure shown in fig. 2, a swap or distillation attempt is now composed of several cut-off attempts. We can write its waiting time M as

$$M = \sum_k \left\{ \left[Y_{\text{cut}}^{(k)} \prod_{j=1}^{k-1} (1 - Y_{\text{cut}}^{(j)}) \right] \cdot \left[Z_s^{(k)} + \sum_{i=1}^{k-1} (Z_f^{(i)}) \right] \right\}$$

This expression will replace $M = \max(T_A, T_B)$ used in eq. (5). For $\tau = \infty$, i.e. no cut-off, Y_{cut} is always 1. Therefore, $k = 1$ is the only surviving term and the two expressions coincide.

To calculate the waiting time distribution, we need three joint distributions: P'_f for unsuccessful input link preparation because of the cut-off, $P'_{s,f}$ for successful preparation but unsuccessful swap/distillation and $P'_{s,s}$ for both successful:

$$\begin{aligned} P'_f(t) &= \Pr(M = t, Y_{\text{cut}} = 0) \\ &= \sum_{t_A, t_B: \min(t_A, t_B) + \tau = t} \Pr(T_A = t_A, T_B = t_B) \cdot [1 - p_{\text{cut}}](T_A, T_B) \end{aligned}$$

$$\begin{aligned} P'_{s,f}(t) &= \Pr(M = t, Y_{\text{cut}} = 1, Y = 0) \\ &= \sum_{t_A, t_B: \max(t_A, t_B) = t} \Pr(T_A = t_A, T_B = t_B) \cdot [p_{\text{cut}} \cdot (1 - p)](t_A, t_B) \end{aligned}$$

$$\begin{aligned} P'_{s,s}(t) &= \Pr(M = t, Y_{\text{cut}} = 1, Y = 1) \\ &= \sum_{t_A, t_B: \max(t_A, t_B) = t} \Pr(T_A = t_A, T_B = t_B) \cdot [p_{\text{cut}} \cdot p](t_A, t_B) \end{aligned}$$

where Y_{cut} and Y describe whether this attempt in CUT-OFF or SWAP/DIST are successful. The prime notation indicates that they describe the waiting time of one attempt in CUT-OFF, in contrast to one attempt in swap or distillation.

For one attempt in swap/distillation with time-out, we then get

$$P_s(t) = \Pr(M = t, Y = 1) = \sum_k \left[\left(\bigstar_{j=1}^{k-1} P'_f(j) \right) * P'_{s,s} \right] (t)$$

$$P_f(t) = \Pr(M = t, Y = 0) = \sum_k \left[\left(\bigstar_{j=1}^{k-1} P'_f(j) \right) * P'_{s,f} \right] (t)$$

The total waiting time then follows using eq. (8).

For entanglement swap, i.e. constant success probability p_{swap} , simplification can be made for this calculation. In this special case, $P'_{s,f}$ and $P'_{s,s}$ differ only by a constant and the same holds for P_s and P_f .

2) *The Werner parameter:* For the Werner parameter, we now need three steps.

We start from calculating the resulting Werner parameter of a swap or distillation for the very last preparation attempt where $Y_{\text{cut}} = Y = 1$. It is denoted by W_{suc} and we only need to replace P_s by $P'_{s,s}$ and $p \cdot w_{\text{out}}$ by $p_{\text{cut}} \cdot p \cdot w_{\text{out}}$ in eq. (9).

Next, we compute the Werner parameter as a function of time that includes the failed cut-off attempts. It is the Werner parameter that the pair of output links of CUT-OFF will produce, given that the swap or distillation operation following is successful. We refer to it as W_{prep} :

$$W_{\text{prep}}(t) = \frac{\sum_{k=1}^{\infty} \left[\left(\bigstar_{j=1}^{k-1} P'_f \right) * (P'_{s,s} \cdot W_{\text{suc}}) \right] (t)}{P_s(t)}.$$

Finally, we consider the time consumed by failed attempts in SWAP or DIST and obtain

$$W_{\text{out}}(t) = \frac{\sum_{k=1}^{\infty} \left[\left(\bigstar_{j=1}^{k-1} P_f \right) * (P_s \cdot W_{\text{prep}}) \right] (t)}{\Pr(T_{\text{out}} = t)}.$$

F. Converting expressions for T_{out} and W_{out} into an efficient algorithm

In the sections above, we presented closed-form expressions for T_{out} and W_{out} for each of the four PROTOCOL-UNITS, as a function of waiting time distribution and Werner parameter of the input links. In order to convert these expressions into an algorithm, we take the same approach as in [18] and cap the infinite sum in eqs. (8) and (10) by a pre-specified truncation time t_{trunc} . This yields a correct $\Pr(T_{\text{out}} = t)$ and $W_{\text{out}}(t)$ for $t \in \{1, \dots, t_{\text{trunc}}\}$ since in each of the expressions with an infinite sum above, $\Pr(T_{\text{out}} = t)$ and $W_{\text{out}}(t)$ are only dependent on waiting time and Werner parameter of input links produced at time $t' \leq t$.

We now show that the algorithm scales polynomially in terms of t_{trunc} . To analyze the complexity, we divide the algorithm into two parts: the iteration over all possible values of T_A , T_B (eqs. (6) and (7)) and the convolution (eqs. (8) and (10)).

The complexity for the first part is $\mathcal{O}(t_{\text{trunc}}^2)$ since it iterates over two discrete random variables up to t_{trunc} . For the second

part, because we need at least one time step in each attempt, i.e. $\Pr(T = 0) = 0$, only the first t_{trunc} convolutions will have non-zero contribution. We can perform the convolution iteratively for each k using at most t_{trunc} convolutions. The complexity of one convolution with fast Fourier transform is $\mathcal{O}(t_{\text{trunc}} \log t_{\text{trunc}})$ [24]. Thus, the complexity of the second part scales as $\mathcal{O}(t_{\text{trunc}}^2 \log t_{\text{trunc}})$. The overall complexity, therefore, is $\mathcal{O}(t_{\text{trunc}}^2 \log t_{\text{trunc}})$.

The preceding discussion shows that the algorithm is efficient as a function of the truncation time. However, for fixed truncation time, the probability mass captured by the algorithm decreases as the number of nodes increases. For protocols without cut-off, variations of the arguments in [18] would allow to prove that the algorithm introduced here is also efficient for fixed probability mass. Unfortunately, the arguments do not translate to protocols with cut-off. This is because for these protocols, the truncation time that covers a fixed probability mass can grow exponentially with the number of nodes, i.e. such an algorithm can not exist.

As example, consider a nested protocol on 2^n repeater segments ($n = 0, 1, 2, \dots$), which for $n = 1$ consists of a GEN block only, and for each additional level $n > 1$, each pair of adjacent links is connected by a CUT-OFF followed by a SWAP. We set $\tau = 0$ for each cut-off, i.e. all elementary links need to be generated at the same time and also all entanglement swaps should succeed at the first attempt for the links to survive all the cut-offs. Since 2^n elementary links need to be generated and the protocol consists of $2^n - 1$ swaps, the probability of successful end-to-end entanglement before time t equals $1 - (1-p)^t$ with $p = p_{\text{gen}}^{N-1} \cdot p_{\text{swap}}^{N-2}$, i.e. decreases exponentially in the number of nodes $N = 2^n + 1$.

IV. OPTIMIZATION

In this section, we describe the details of our optimization over cut-offs, including the figure of merit and optimization method.

In our numerical study, we use the secret-key rate of the BB84 protocol [25] as a figure of merit to assess the performance of composite repeater protocols. We compute the secret-key rate R as the secret-key fraction divided by the average waiting time

$$R = \frac{r}{\bar{T}}. \quad (13)$$

The secret-key fraction r describes the amount of secret key that can be extracted from the generated entanglement and is given by [26], [27]

$$r(w) = \max \{0, 1 - h[e_X(w)] - h[e_Z(w)]\}$$

where $h(p) = -p \log_2(p) - (1-p) \log_2(1-p)$ is the binary entropy function and e_X (e_Z) is the quantum bit error rate in the X (Z) basis. Since the quantum states tracked by our algorithm are Werner states at any point in the execution of the composite repeater protocol (see section II), the quantum bit error rate can be expressed as function of the end-to-end state's Werner parameter:

$$e_Z(w) = \langle 01 | \rho(w) | 01 \rangle + \langle 10 | \rho(w) | 10 \rangle = \frac{1-w}{2}$$

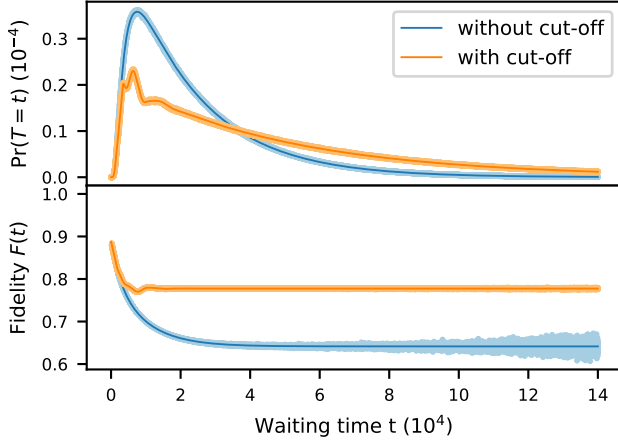


Fig. 4. The probability distribution of the waiting time T and the average fidelity $F(t)$ of the end-to-end link for a protocol with and without a cut-off (solid lines) for a 9-node repeater protocol of the form as in eq. (14) (unit of time is the attempt duration of elementary link generation, L_0/c). We observe that the fidelity increases for most times t while the probability that the link is produced at time t shifts to larger t , indicating longer waiting time. The secret-key rates computed from the data are 0 (without cut-off) and $0.32 \cdot 10^{-5}$ (with cut-off). The parameters used are $p_{\text{gen}} = 10^{-3}$, $p_{\text{swap}} = 0.5$, $w_0 = 0.98$, $t_{\text{coh}} = 4 \cdot 10^4$ and the cut-offs for the three nesting levels are $\tau = (1700, 3200, 5500)$ (in increasing order of number of segments spanned by the CUT-OFF block). Computation time ≈ 2 hours. We observe good agreement with a Monte Carlo algorithm (dots), which we use for validating correctness of our implementation (see appendix A for details).

for a Werner state $\rho(w)$ defined in eq. (1). The same result holds for e_X because of the symmetry of the Werner state. In appendix B, we detail how we compute the secret-key rate with truncated waiting time distribution and Werner parameter obtained from the algorithm in section III-F.

Since the memory cut-off time is discrete ($\tau \in \{0, 1, 2, \dots, t_{\text{trunc}}\}$), we need an optimization algorithm which is compatible with a discrete search space. We choose the differential evolution algorithm implemented in the SciPy-optimization library of the Python programming language [28], [29].

V. NUMERICAL RESULTS

In this section, we optimize over repeater protocols with cut-offs in order to maximize the rate at which secret key can be extracted from the produced end-to-end entanglement. We arrive at the improved secret-key rate as follows: first, we use our algorithm from section III to show that the use of a cut-off boosts secret-key rate. Then, we optimize the secret-key rate over the choice of cut-off value for a range of hardware parameters and show that the resulting repeater protocols produce secret key at significantly higher rates than their no-cut-off alternatives. We finish by analyzing the sensitivity of the achievable secret-key rate at the optimal cut-off with respect to the hardware parameters.

We investigate repeater protocols with 3 nesting levels where at each nesting level the range of entanglement is doubled by an entanglement swap. The protocol thus spans $2^3 = 8$ segments ($8 + 1 = 9$ nodes). Each entanglement swap

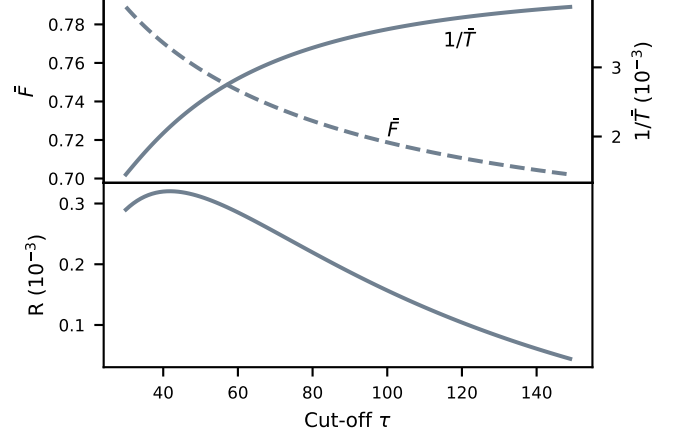


Fig. 5. Influence of choice of cut-off on average waiting time, average fidelity and secret-key rate for repeater protocols of the form eq. (14). **(Top)** Increasing the cut-off yields higher average generation rate (reciprocal of average waiting time \bar{T}) but lower average fidelity \bar{F} . **(Bottom)** The secret key rate R as a function of the cut-off time. The used parameters are $p_{\text{gen}} = 0.1$, $p_{\text{swap}} = 0.5$, $w_0 = 0.98$ and $t_{\text{coh}} = 400$. The chosen truncation time is 4000. Cut-off time is chosen identical for all three swap levels. Unit of time is the attempt duration of elementary link generation.

operation is preceded by a cut-off, i.e. the scheme is of the form

$$\text{GEN} \rightarrow (\rightarrow \text{CUT-OFF} \rightarrow \text{SWAP})^3. \quad (14)$$

The numerical results in this section were obtained using our open-source implementation [30] of the algorithm from section III on consumer-market hardware (Intel i7-8700 CPU and NVIDIA GTX 1070 GPU). We validated correctness of the implementation by comparison with an extended version of the Monte Carlo algorithm from [18] (see fig. 4 and appendix A for details).

Using the implementation, we compute waiting time and average fidelity for a particular choice of cut-off at each of the three levels and compare it with the protocol without cut-off (cut-off duration $\tau = \infty$ at each nesting level), see fig. 4. We observe that the cut-off increases fidelity at the cost of longer waiting time, as one would intuitively expect. We further quantify the time-fidelity trade-off for a range of cut-offs in fig. 5. For maximizing the secret key rate, we observe a single optimal choice of the cut-off τ .

We proceed with optimizing the cut-off to maximize secret key rate for a range of parameters. The best secret-key rates one can get with cut-offs for different repeater parameters are shown in fig. 6(a-d). We observe that cut-offs extend the parameter regime for which secret key can be generated. To see how much one can gain in the secret key rate by using cut-offs, we choose two parameters t_{coh} and w_0 and plot the absolute increase in fig. 7. We observe that the use of the optimal cut-off increases the secret key rate for the entire parameter range plotted and the improvement is largest close to the threshold parameters at which the no-cut-off protocol starts to produce nonzero secret key.

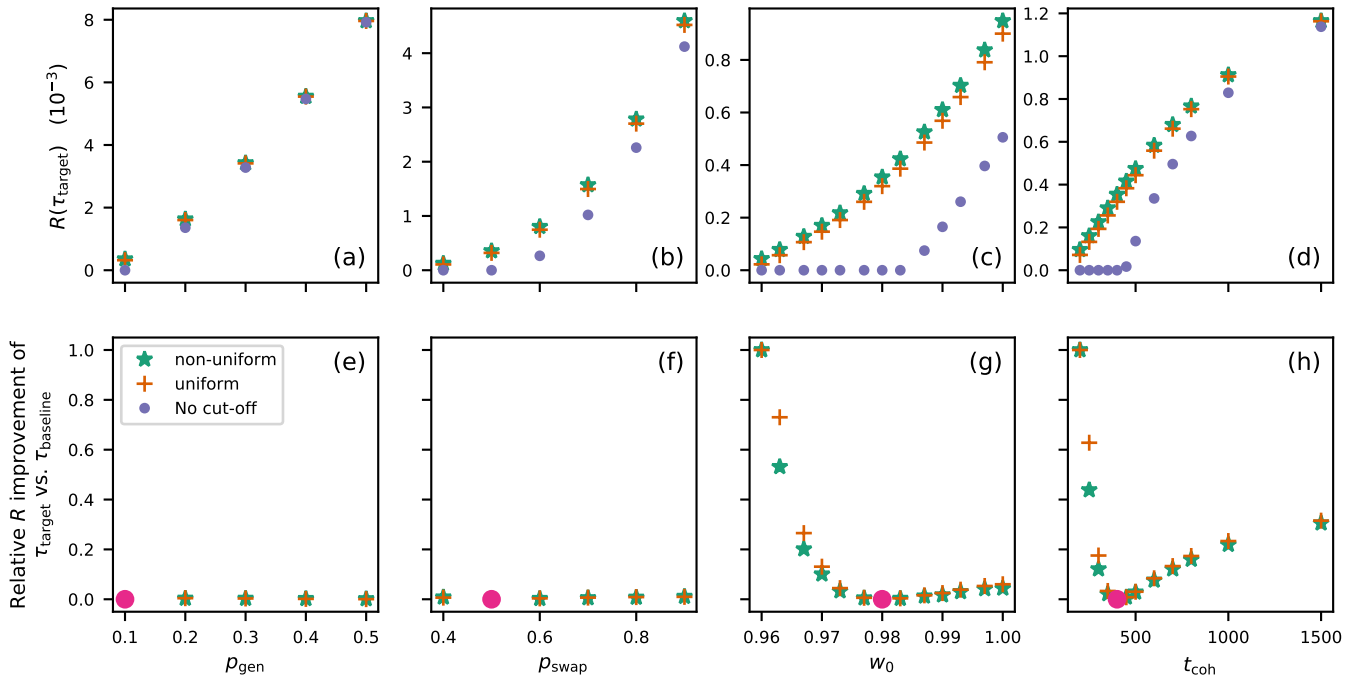


Fig. 6. The effect of the optimal cut-off on secret-key rate for different hardware parameters, for the 9-node protocol as in eq. (14). We choose a set of parameters as baseline parameters ($p_{\text{gen}} = 0.1$, $p_{\text{swap}} = 0.5$, $w_0 = 0.98$ and $t_{\text{coh}} = 400$) and in each plot in the figure, we vary only one of the four parameters. The **top plots (a-d)** show the performance of the protocol with optimized cut-offs, where the optimization is implicitly performed for each data point separately. The set of cut-offs we optimize over is either non-uniform (allow for different cut-offs at the three nesting levels of the protocols) or uniform (same cut-off at each level). We observe that the performance difference between uniform and non-uniform cut-offs is small or even negligible. The plots also indicate parameter regimes in which the protocol with the optimal cut-off generates key while its no-cut-off alternative does not (i.e. the no-cut-off has zero secret-key rate). The **bottom plots (e-h)** show relative performance improvement (eq. (15)) of the optimal cut-off (τ_{target}) for a given data point, versus the optimal cut-off τ_{baseline} for the baseline parameters (see above). The plots show that cut-off performance is greatly sensitive to coherence time (t_{coh}) and elementary link quality (w_0), while it is barely influenced by varying success probabilities of elementary-link generation (p_{gen}) and entanglement swapping (p_{swap}). Note that the smaller the relative secret-key rate improvement (vertical axis), the closer the performance of τ_{baseline} is to the performance of the optimal τ_{target} , which is why in the plots the best-performing ‘non-uniform’ cut-off shows smaller relative improvement than the best-performing ‘uniform’ cut-off. The purple circles refer to the baseline parameters.

In addition, we compare uniform and non-uniform cut-offs, where ‘uniform’ means that we choose the same cut-off time for each nesting level. For the parameter regimes studied, we observe that non-uniform and uniform cut-off perform similarly, see fig. 6(a-d).

Our next step is the sensitivity analysis of cut-off performance in the hardware parameters. For this, we first choose baseline values for the four hardware parameters and find the corresponding optimal cut-off τ_{baseline} . Given a target set of parameters that deviates slightly from the baseline values (optimal cut-off τ_{target}), we quantify the sensitivity by their relative performance difference

$$\frac{R(\tau_{\text{target}}) - R(\tau_{\text{baseline}})}{R(\tau_{\text{target}})} \quad (15)$$

where R is the secret-key rate achieved by the repeater protocol. If this relative difference is small, the performance of the baseline cut-off is insensitive to the parameter deviation. In fig. 6(e-h), we plot the relative performance difference for deviations in each of the four hardware parameters separately. We find that the performance of the baseline cut-off is greatly influenced by variation in of coherence time and elementary

link quality, but not so much by the success probabilities of elementary link generation and swapping.

VI. CONCLUSION

In this work, we optimized the secret key rate over repeater protocols including cut-offs. Our main tool is an algorithm for computing the probability distribution of waiting time and fidelity of the first generated end-to-end link. The algorithm is applicable to a large class of quantum repeater schemes that can include cut-off strategies and distillation. Its runtime is polynomial in the support size of the probability distribution of waiting time.

Our simulations show that the use of the optimal cut-off lowers the hardware quality threshold at which secret key can be generated compared to the no-cut-off alternative. Furthermore, we observed an increase in secret-key rate for the entire regime studied for which the no-cut-off protocol produces nonzero key.

Regarding the choice of cut-off, we find that uniform cut-offs lead to a negligible reduction in the secret key rate compared to the optimal set of cut-offs which differ per nesting level. Moreover, the optimal uniform cut-off is highly sensitive to the quality of the memory and of the elementary links, while

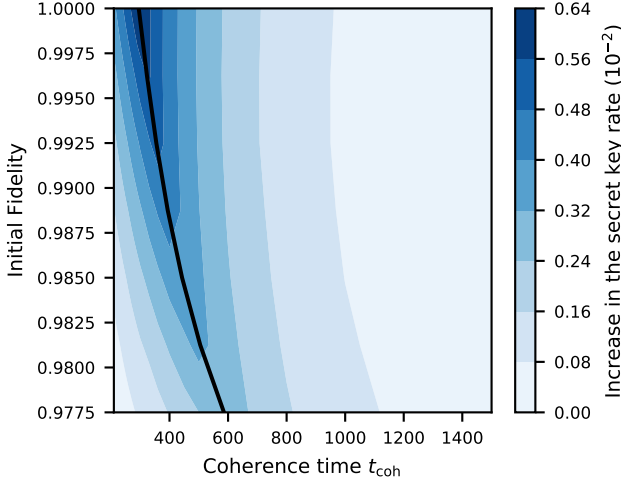


Fig. 7. Absolute increase in secret key rate with the optimal cut-off compared to no cut-off as a function of memory coherence time and fidelity of the elementary links ($= (1 + 3w_0)/4$, see section II), for the 9-node repeater protocols as in eq. (14). The black solid line separates the area where the no-cut-off protocol produces no secret key (left of line) and where its secret-key rate is strictly larger than zero (right of line). We observe that for the entire parameter range depicted in the figure, cut-offs increase the secret key rate and the absolute improvement is largest for parameters close to the key-producing threshold for the no-cut-off protocol (i.e. close to the black solid line). The plot consists of 140 data points on a grid and the used parameters are $p_{\text{gen}} = 0.1$ and $p_{\text{swap}} = 0.5$. Time unit is the duration of a single elementary link generation attempt.

it is barely influenced by the success probabilities for swapping and elementary link generation. Such sensitivity could guide the heuristic cut-off optimization of more complex protocols.

ACKNOWLEDGMENT

The authors would like to thank Sebastiaan Brand, Kenneth Goodenough and Filip Rozpędek for helpful discussions. This work was supported by the QIA project (funded by European Union's Horizon 2020, Grant Agreement No. 820445) and by the Netherlands Organization for Scientific Research (NWO/OCW), as part of the Quantum Software Consortium program (project number 024.003.037 / 3368). Boxi Li is supported by the IDEA League student grant programme.

APPENDIX

APPENDIX A

VALIDATION AGAINST A MONTE CARLO ALGORITHM

In this section, we verify that our implementation of the deterministic algorithm presented in section III is correct by validation against the Monte Carlo sampling algorithm from Brand et al. [18]. For all repeater schemes we ran (up to $2^{10} + 1$ nodes for some parameters), we observed good agreement between the waiting time probability distribution and Werner parameter the algorithms computed, which is convincing evidence that our implementation is correct. Fig. 4 depicts the result of a typical run.

What follows is a brief description of the Monte Carlo algorithm from Brand et al. [18], including an extension to

CUT-OFF. Each run of the Monte Carlo algorithm samples a tuple of waiting time and Werner parameter. It is defined recursively by having a dedicated function for each PROTOCOL-UNIT (described below) call the dedicated functions of the two PROTOCOL-UNITs that produce its two input links. The recursion follows the repeater protocol's tree structure (see fig. 1), resulting in a sampling algorithm of waiting time and Werner parameter of the entire repeater protocol.

The dedicated functions for each of the four PROTOCOL-UNITs are as follows. If the protocol is only a GEN, the Monte Carlo algorithm samples the waiting time from the geometric distribution with parameter p_{gen} and the Werner parameter is the constant w_0 . For the other PROTOCOL-UNITs, each of which takes two links as input, the algorithm begins by initializing the total elapsed time $t = 0$. Then, it enters a loop which starts by calling the dedicated functions of the PROTOCOL-UNITs that produce the two input links, resulting in two samples (t_A, w_A) and (t_B, w_B) . The algorithm randomly declares 'success' or 'failure' according to the success probability in table I. If it succeeds, the function breaks the loop and outputs $t + \max(t_A, t_B)$ and the resulting Werner parameter $w_{\text{out}}(t_A, w_A, t_B, w_B)$ (see table I). If it fails, the total elapsed time t is increased by the waiting time ($\max(t_A, t_B)$ for SWAP and DIST, $\min(t_A, t_B) + \tau$ for CUT-OFF) and the function goes back to the start of the loop.

APPENDIX B

CALCULATION OF THE SECRET-KEY RATE

Here, we show how we calculate the secret-key rate with truncated waiting time distribution.

One could think of the secret-key rate, computed with finite truncation time $t_{\text{trunc}} < \infty$, as an approximation of the real secret-key rate or, alternatively, as the rate achieved by the following repeater protocol. The protocol starts with the two parties at the end nodes agree on a truncation time t_{trunc} . If up to $t = t_{\text{trunc}}$ the end-to-end link has not been delivered, the protocol terminates and restarts from GEN. Therefore, the number of protocol executions follows the geometric distribution with success probability $p_{\text{tr}} = \Pr(T \leq t_{\text{trunc}})$. The waiting time for a failed protocol is t_{trunc} while for a successful one it follows the waiting time distribution $\Pr(T = t)$ for $t < t_{\text{trunc}}$. The average total waiting time is then the sum of the time consumed in failed and successful executions:

$$\bar{T} = t_{\text{trunc}} \cdot \left(\sum_{k=1}^{\infty} k \cdot p_{\text{tr}}(1 - p_{\text{tr}})^k \right) + \frac{\sum_{t=1}^{t_{\text{trunc}}} t \cdot \Pr(T = t)}{\Pr(T \leq t_{\text{trunc}})}$$

Accordingly, the average Werner parameter is an average over the successful execution

$$\bar{W} = \frac{\sum_{t=1}^{t_{\text{trunc}}} W(t) \cdot \Pr(T = t)}{\Pr(T \leq t_{\text{trunc}})}.$$

With the above equations, we calculate the secret-key rate defined in eq. (13). In this work, we choose heuristically a t_{trunc} such that $\Pr(T \leq t_{\text{trunc}}) \geq 99\%$. With this choice, the difference in the secret key rate between protocols with finite and infinite t_{trunc} is negligibly small.

REFERENCES

- [1] H. J. Kimble, “The quantum internet,” *Nature*, vol. 453, no. 7198, p. 1023, 2008. [Online]. Available: <https://doi.org/10.1038/nature07127>
- [2] S. Wehner, D. Elkouss, and R. Hanson, “Quantum internet: A vision for the road ahead,” *Science*, vol. 362, no. 6412, 2018. [Online]. Available: <https://science.sciencemag.org/content/362/6412/eaam9288>
- [3] H.-J. Briegel, W. Dür, J. I. Cirac, and P. Zoller, “Quantum repeaters: The role of imperfect local operations in quantum communication,” *Phys. Rev. Lett.*, vol. 81, pp. 5932–5935, Dec 1998. [Online]. Available: <https://link.aps.org/doi/10.1103/PhysRevLett.81.5932>
- [4] W. J. Munro, K. Azuma, K. Tamaki, and K. Nemoto, “Inside quantum repeaters,” *IEEE Journal of Selected Topics in Quantum Electronics*, vol. 21, no. 3, pp. 78–90, may 2015. [Online]. Available: <https://doi.org/10.1109/JSTQE.2015.2392076>
- [5] S. Muralidharan, L. Li, J. Kim, N. Lütkenhaus, M. D. Lukin, and L. Jiang, “Optimal architectures for long distance quantum communication,” *Scientific reports*, vol. 6, p. 20463, 2016. [Online]. Available: <https://doi.org/10.1103/PhysRevLett.98.060502>
- [6] O. A. Collins, S. D. Jenkins, A. Kuzmich, and T. A. B. Kennedy, “Multiplexed memory-insensitive quantum repeaters,” *Phys. Rev. Lett.*, vol. 98, p. 060502, Feb 2007. [Online]. Available: <https://link.aps.org/doi/10.1103/PhysRevLett.98.060502>
- [7] L. Praxmeyer, “Reposition time in probabilistic imperfect memories,” *arXiv:1309.3407*, 2013. [Online]. Available: <https://arxiv.org/abs/1309.3407>
- [8] N. Kalb, A. A. Reiserer, P. C. Humphreys, J. J. W. Bakermans, S. J. Kamerling, N. H. Nickerson, S. C. Benjamin, D. J. Twitchen, M. Markham, and R. Hanson, “Entanglement distillation between solid-state quantum network nodes,” *Science*, vol. 356, no. 6341, pp. 928–932, jun 2017. [Online]. Available: <https://doi.org/10.1126/Science.aan0070>
- [9] F. Rozpędek, R. Yehia, K. Goodenough, M. Ruf, P. C. Humphreys, R. Hanson, S. Wehner, and D. Elkouss, “Near-term quantum-repeater experiments with nitrogen-vacancy centers: Overcoming the limitations of direct transmission,” *Phys. Rev. A*, vol. 99, p. 052330, May 2019. [Online]. Available: <https://link.aps.org/doi/10.1103/PhysRevA.99.052330>
- [10] F. Rozpędek, K. Goodenough, J. Ribeiro, N. Kalb, V. C. Vivoli, A. Reiserer, R. Hanson, S. Wehner, and D. Elkouss, “Parameter regimes for a single sequential quantum repeater,” *Quantum Science and Technology*, 2018. [Online]. Available: <http://iopscience.iop.org/10.1088/2058-9565/aab31b>
- [11] S. Santra, L. Jiang, and V. S. Malinovskiy, “Quantum repeater architecture with hierarchically optimized memory buffer times,” *Quantum Science and Technology*, vol. 4, no. 2, p. 025010, mar 2019. [Online]. Available: <https://doi.org/10.1088/2058-9565/2Fab0bc2>
- [12] K. Chakraborty, F. Rozpędek, A. Dahlberg, and S. Wehner, “Distributed routing in a quantum internet,” *arXiv:1907.11630*, 2019. [Online]. Available: <https://arxiv.org/abs/1907.11630>
- [13] P. van Loock, W. Alt, C. Becher, O. Benson, H. Boche, C. Deppe, J. Eschner, S. Höfling, D. Meschede, P. Michler, F. Schmidt, and H. Weinfurter, “Extending quantum links: Modules for fiber- and memory-based quantum repeaters,” *arXiv:1912.10123*, 2019. [Online]. Available: <https://arxiv.org/abs/1912.10123>
- [14] F. Schmidt and P. van Loock, “Memory-assisted long-distance phase-matching quantum key distribution,” *arXiv:1910.03333*, 2019. [Online]. Available: <https://arxiv.org/abs/1910.03333>
- [15] S. Khatri, C. T. Matyas, A. U. Siddiqui, and J. P. Dowling, “Practical figures of merit and thresholds for entanglement distribution in quantum networks,” *Phys. Rev. Research*, vol. 1, p. 023032, Sep 2019. [Online]. Available: <https://link.aps.org/doi/10.1103/PhysRevResearch.1.023032>
- [16] E. Shchukin, F. Schmidt, and P. van Loock, “Waiting time in quantum repeaters with probabilistic entanglement swapping,” *Phys. Rev. A*, vol. 100, p. 032322, Sep 2019. [Online]. Available: <https://link.aps.org/doi/10.1103/PhysRevA.100.032322>
- [17] Y. Wu, J. Liu, and C. Simon, “Near-term performance of quantum repeaters with imperfect ensemble-based quantum memories,” *Phys. Rev. A*, vol. 101, p. 042301, Apr 2020. [Online]. Available: <https://link.aps.org/doi/10.1103/PhysRevA.101.042301>
- [18] S. Brand, T. Coopmans, and D. Elkouss, “Efficient computation of the waiting time and fidelity in quantum repeater chains,” *IEEE Journal on Selected Areas in Communications*, pp. 1–1, 2020. [Online]. Available: <https://ieeexplore.ieee.org/document/8972391>
- [19] M. Żukowski, A. Zeilinger, M. A. Horne, and A. K. Ekert, “Event-ready-detectors” Bell experiment via entanglement swapping,” *Phys. Rev. Lett.*, vol. 71, pp. 4287–4290, Dec 1993. [Online]. Available: <https://link.aps.org/doi/10.1103/PhysRevLett.71.4287>
- [20] C. H. Bennett, G. Brassard, S. Popescu, B. Schumacher, J. A. Smolin, and W. K. Wootters, “Purification of noisy entanglement and faithful teleportation via noisy channels,” *Phys. Rev. Lett.*, vol. 76, pp. 722–725, Jan 1996. [Online]. Available: <https://link.aps.org/doi/10.1103/PhysRevLett.76.722>
- [21] D. Deutsch, A. Ekert, R. Jozsa, C. Macchiavello, S. Popescu, and A. Sanpera, “Quantum privacy amplification and the security of quantum cryptography over noisy channels,” *Phys. Rev. Lett.*, vol. 77, pp. 2818–2821, Sep 1996. [Online]. Available: <https://link.aps.org/doi/10.1103/PhysRevLett.77.2818>
- [22] W. Dür, H.-J. Briegel, J. I. Cirac, and P. Zoller, “Quantum repeaters based on entanglement purification,” *Phys. Rev. A*, vol. 59, pp. 169–181, Jan 1999. [Online]. Available: <https://link.aps.org/doi/10.1103/PhysRevA.59.169>
- [23] R. F. Werner, “Quantum states with Einstein-Podolsky-Rosen correlations admitting a hidden-variable model,” *Phys. Rev. A*, vol. 40, pp. 4277–4281, Oct 1989. [Online]. Available: <https://link.aps.org/doi/10.1103/PhysRevA.40.4277>
- [24] J. W. Cooley and J. W. Tukey, “An algorithm for the machine calculation of complex fourier series,” *Mathematics of Computation*, vol. 19, no. 90, p. 297, apr 1965. [Online]. Available: <https://doi.org/10.2307/2F2003354>
- [25] C. H. Bennett and G. Brassard, “Quantum cryptography: Public key distribution and coin tossing,” *Proceedings of IEEE International Conference on Computers, Systems and Signal Processing*, vol. 175, 1984. [Online]. Available: <https://doi.org/10.1016/j.tcs.2014.05.025>
- [26] P. W. Shor and J. Preskill, “Simple proof of security of the BB84 quantum key distribution protocol,” *Phys. Rev. Lett.*, vol. 85, pp. 441–444, Jul 2000. [Online]. Available: <https://link.aps.org/doi/10.1103/PhysRevLett.85.441>
- [27] H.-K. Lo, H. F. Chau, and M. Ardehali, “Efficient quantum key distribution scheme and a proof of its unconditional security,” *Journal of Cryptology*, vol. 18, no. 2, pp. 133–165, 2005. [Online]. Available: <https://doi.org/10.1007/s00145-004-0142-y>
- [28] R. Storn and K. Price, “Differential evolution—a simple and efficient heuristic for global optimization over continuous spaces,” *Journal of global optimization*, vol. 11, no. 4, pp. 341–359, 1997. [Online]. Available: <https://doi.org/10.1023/A:1008202821328>
- [29] P. Virtanen, R. Gommers, T. E. Oliphant, M. Haberland, T. Reddy, D. Cournapeau, E. Burovski, P. Peterson, W. Weckesser, J. Bright *et al.*, “SciPy 1.0: fundamental algorithms for scientific computing in Python,” *Nature methods*, pp. 1–12, 2020. [Online]. Available: <https://doi.org/10.1038/s41592-019-0686-2>
- [30] “Optimization of cut-offs for repeater chains,” <https://github.com/BoxiLi/repeater-cut-off-optimization>, 2019.